CHAPTER-IV

CHAPTER - IV

ELECTRICAL, OPTICAL, AND STRUCTURAL PROPERTIES OF CdS AND CdS:Sb THIN FILMS

4.1 Introduction

The essentials of photoelectrochemical cells comprising three components (viz, a photoelectrode, an electrolyte, and a counter electrode) are summarised in Chapter - I. The basics involved in thin film deposition processes, nature of the semiconductor/electrolyte interface, and charge transport reactions in dark and in lighted conditions have been briefly outlined in Chapter-II. The know-how of a chemical deposition process, the experimental deposition conditions, preparative parameters, and the actual details of procedure for the preparation of CdS and CdS:Sb thin films have been discussed in Chapter-III. The growth mechanism is also discussed.

As our main intention is to obtain an acceptable output power from a photoelectrochemical cell, characterization of the semiconductor material in thin film form is essential. Now it has been well known that the properties of a semiconductor/electrolyte interface are sensitive function of the properties of a photoelectrode material [67] i.e. the effective performance of a photoeletrochemical cell is found to rely on the photoelectrode properties. Thus the prehistory of a photoelectrode material is a need to know. Any change in the properties of photoelectrode material alters both the electrical and the optical properties of a photoelectrochemical cell.Especially the charge transfer rate across the interface, generation of the short circuit current, I_{sc} and open circuit voltage, V_{oc}, a

photoelectrochemical cell are closely related to the material (semiconductor) properties, an electrolyte, and the nature of the junction between them. Thus the detailed analysis of a photoelectrode material is highly advisable. This chapter is an attempt to study the electrical, optical, and structural properties of the CdS and CdS:Sb thin films. The necessary design and fabrication of the characterization tools have also been mentioned. Since cadmium sulphide films are prepared by a chemical deposition process the preparative parameters and deposition conditions like deposition temperature, speed of the substrate rotation, molar concentration of the reactants, deposition time, substrate holder geometry etc affect the growth mechanism reflecting into the quality and physical appearance of the samples. The above preliminary conditions are stabilised in the first few stages of the work and are listed in brief in section 4.3.1.

Generally films deposited using this technique are highly resistive. The initial high resistivity can be lowered considerably by maintaining proper ratio of Cd^{2+} and S^{2-} [94-96]. The Cd:S ratio selected in this work is 1:1 [95-97]. The resistivity can be further decreased by doping with trivalent impurity as suggested by many workers [43,97-100].

Section 4.3.2 and 4.3.3 reveals respectively the effects of antimony doping on various properties of the CdS films.

4.2 Experimental Details

Cadmium sulphide thin films were prepared by our modified chemical deposition process onto amorphous glass substrates by keeping Cd:S ion ratio as 1.1 as per the procedure outlined in section 3.5. The doping concentration of trivalent antimony was changed from 0.005 wt % to 1 Wt %. The films were preserved in an air tight dark desicator. The various experimental measurements carried out with these films are as below.

4.2.1 Measurement of thickness.

The thickness of all the samples was measured by following weight difference density considerations. The method involves measurement of mass, area, and density of the material. The density of the material is related to its area and mass as;

$$t = \frac{m}{A.d} \qquad \text{.....(4.1)}$$

Where, m = Weight in grams of the film.

A = area in Cm^2 of the film.

d = density of the material (4.8 gm/cm^3 for CdS)

4.2.2 Electrical properties.

a) Design and fabrication of conductivity measuring unit and measurment of conductivity:

The dark conductivity of the samples was measured by using a conductivity measuring unit as shown in fig.4.1 designed in our laboratory [43].

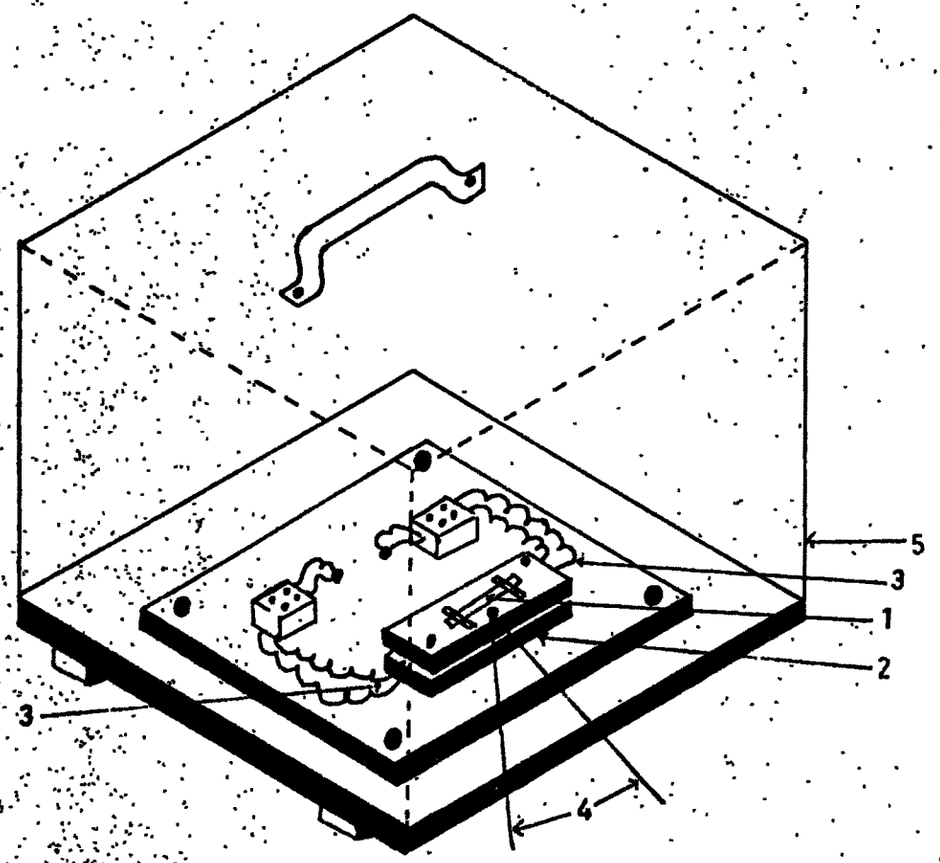

Fig.4.1 An experimental arrangement for the measurement of conductivity.

1. Sample.
2. Brass plates
3. Electrical heaters
4. Thermocouple
5. Shield.

It consists of two brass plates of the size 10 x 5 x 0.6 cm. One of the plate is fixed tightly on a asbestos base of the dimension 10 x 10 inches. Two strip heaters (65 Watt) were kept in parallel on the first brass plate and other plate was fixed tightly to the lower plate. i.e. strip heaters were sandwiched in between the two brass plates to achieve the uniform temperature. A mica sheet was used to wrap the heaters before being put in between the brass plates so as to achieve the electrical insulation for either of the brass plates. A sample holder of the dimension 3 x 0.5 x 0.6 cm. was designed and fixed permanently exactly at the centre of the upper plate A. Sample whose conductivity was to be measured was mounted with a copper press contacts below the sample holder. The sample was electrically insulated from upper brass plates and the sample holder by interposing the mica pieces at the proper places. Thermal radiation losses were reduced by covering the whole set up in a bakelite box. The box was coated from inside by the asbestoss sheets. The working temperature was recorded with a Chromel Alumel thermocouple (24 guage) fitted at the centre on the top of the upper plate. The Aplab TPSU (Transistorised Power Supply Unit) was used to pass the current through the sample. The potential drop across the sample was measured with the help of digital multimeter (pla-

DM-14B) and current through the sample was noted with a sensitive HIL - 2665, 4½ digit nanoammeter.

b) Design and fabrication of thermoelectric power (TEP) unit and measurement of TEP :

The necessary conditions and requirements for thermoelectric power measurement such as maximum temperature difference and minimum contact resistance have been discussed by Bauerie et.al. [101]. The necessary care was taken to fulfil the above requirements while fabricating the thermoelectric power unit. Fig. 4.2 shows a schematic of the TEP measurement unit. It consists of two copper plates of the dimension 5 x 4 x 1.2 cm fitted on a asbestos sheet supported by a bakelite sheet. The plates were arranged in parallel separated by a distance of 0.5 cm. The plates were pitched to a size of the miniheaters, from the bottom and the miniheaters of the different wattage (65 W and 35 W) were fixed in them. Care was taken of the elctrical insulation between the miniheaters and the copper plates by means of a mica sheet. A pair of sample holder was fabricated in our laboratory in a similar fashion as that of the conductivity measurement and fixed on the top adjuscent nearer edges of the copper block lengthwise. The sample size used in this study was 2.5 x 0.5 cm. on amorphous glass substrate and the dimensions of the substrate holder were 3 x 0.5 x

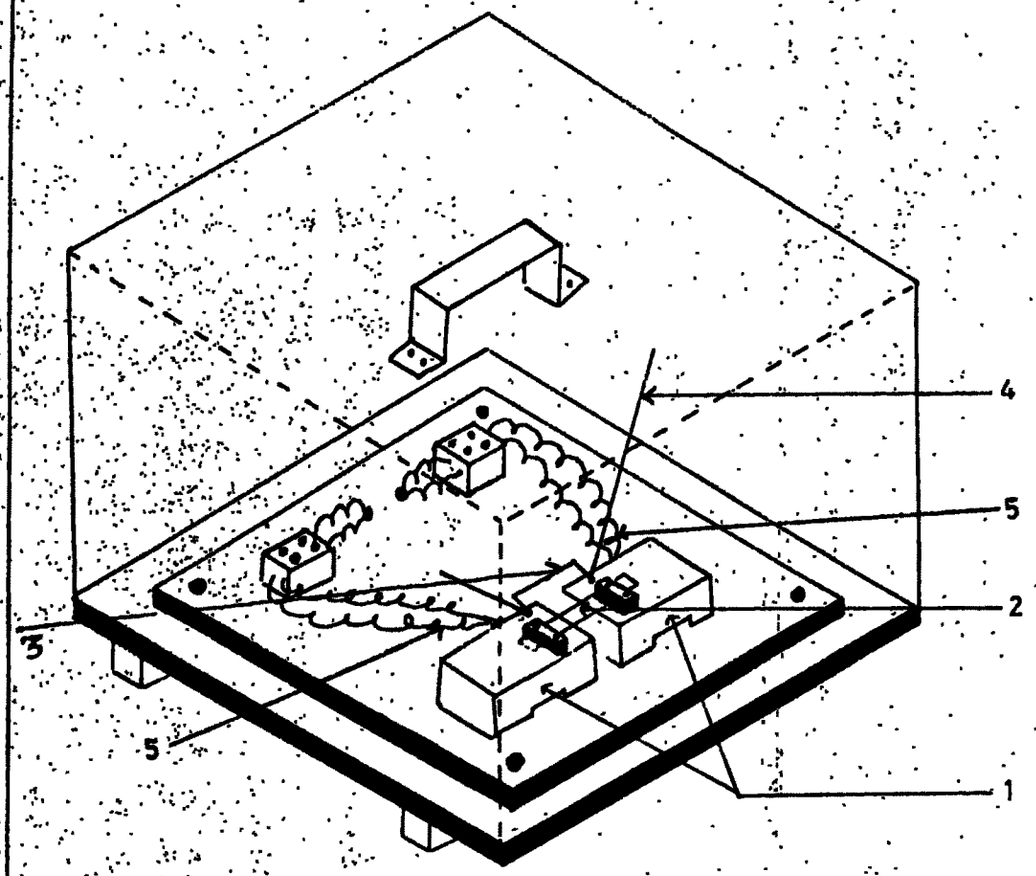

Fig.4.2 Thermoelectric power measuring unit.

1. Copper blocks.
2. Sample.
3. Thermocouple (Mean temperature recorder).
4. Differential thermocouple (Thermovoltage recorder)
5. Heaters.

0.5 cms. The sample was electrically insulated from copper blocks and the substrate holder by means of mica pieces. The press copper contacts were used for the measurement. Chromel-Alumel thermocouples (24 guage) were fixed on the top of the copper blocks for the temperature measurement. The proper shielding of a unit was made by a bakelite box to minimize the losses due to thermal radiations. Thermovoltage was measured by a $4^1/2$ digit, HIL-2665 micro-voltmeter. The temperature gradient measurement was done with $3^1/2$ digit, Agronic -113 DC microvoltmeter.

4.2.3 Optical properties :

To know the type of transition and to estimate the optical absorbance and forbidden energy gap of the material, the optical absorption measurements have been carried out. Both doped and undoped samples of cadmium sulphide were scanned for the optical absorption studies in which optical density was measured as a function of wavelength. The photospectrometer, Hitachi Japan, was utilised to persue this measurements. Scanning rate was 100 nm per minute and the range of wavelength was 400 nm to 900 nm.

4.2.4 Structral properties :

a) SEM Studies :

Scanning Electron Microscopy (SEM) studies of the samples were obtained from, RSIC, Nagpur for the

thin film samples. The resolution selected was 11000.

b) XRD studies :

The XRD studies on thin film samples were examined by using Phillips PW - 1710 X-ray diffractometer with CuK_{α} - radiations.

4.3 Results and Discussion :

Preparation of thin film photoactive materials play an important role in devising photoelectrochemical solar cells. Thin film photoactive electrodes have the overriding advantages of ease of preparation and cheapness because of the very small quantity of the active materials required. A quality thin film material results, if number of preparative parameters such as, deposition temperature, deposition time, speed of substrate rotation, pH, and concentration of basic ingradients etc are optimised. Following are the possible parameters studied in brief while depositing the samples.

4.3.1 Finalisation of deposition conditions :

The thin films of cadmium sulphide have been prepared by a solution growth technique. The mechanism and process of film formation from cadmium sulphate and thiourea with liquor ammonia as a complexing agent is discussed in section 3.4. Ammonia forms a complex compound (cadmium tetra ammonium sulphate) with cadmium sulphate. The dissociation of thiourea occurs in this alkaline medium when temperature

of the reaction vessel is raised to 85°C to form the bivalent sulphide ions which then react with complex ions to form CdS nucleus.

$$Cd(NH_3)_4^{2+} + S^{2-} \longrightarrow CdS + 4\,NH_3 \uparrow$$

The process of formation of CdS films is found to be a strong function of various preparative parameters and deposition conditions. The various parameters overviewed are

(a) Deposition temperature.

The deposition temperature plays an important role while preparing the CdS samples. In a reaction vessel there is no solid phase of $Cd(OH)_2$ to speed up the decomposition of thiourea. As a result film formation is expected to take place above a certain temperature. Thermal energy helps to decompose thiourea and also provides kinetic energy to the ions resulting into an increased number of collisions and hence the film formation occurs. The films were deposited at various temperatures, at an interval of 10°C. The physical appearance of the samples such as uniformity, stickness, thickness etc. showed that the films deposited at 85°C are more suitable relative to others.

(b) Deposition time.

As thiourea decomposes slowly the deposition of CdS films is a slow process. Further, it is reported that the deposition at 85°C results in uniform and best

quality films [95], and a saturation in film thickness is observed after 40 minutes. A deposition time of approximately 45 minutes was selected to ensure the maximum thickness [95].

(c) Geometry of the substrate holder.

A substrate holder designed in our laboratory (section 3.2.4) was used to fix the position of the rotating samples. It was found that the substrates at 90° each other gave uniform deposits implying that the geometry of the substrate holder allows required crystal orientation [95]. A substrate holder in which substrates make an angle of 90° with the respective diameter is used in further study.

(d) Speed of the substrate rotation.

The speed of the rotation of the substrates is the key factor in deciding the thickness of the deposit. An uniform speed of substrate rotation was varied with the help of constant speed ac gear motor from 50 r.p.m. to 150 r.p.m. It was found that the deposit thickness goes on decreasing as the speed increases as shsown in fig. 4.3. For any speed in low speed range (50 to 65 r.p.m.) films are found to be thick, nonspecular and spotty while in the medium range of speeds (70 to 90 r.p.m.) thick, diffused, and adhesive deposits are obtained. At higher speed of rotation films are specularly reflecting and adhesive. Attempts were made further to deposit the

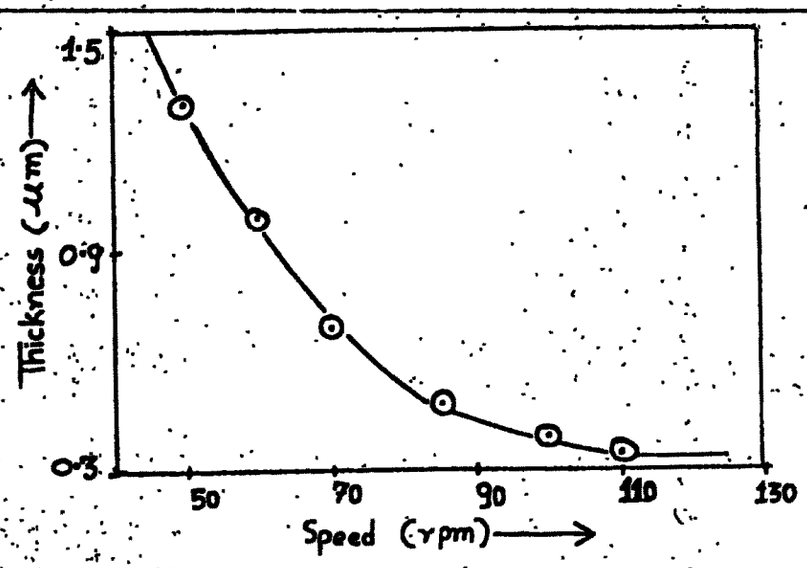

Fig.4.3 Dependence of film thickness on speed of the substrate rotation.

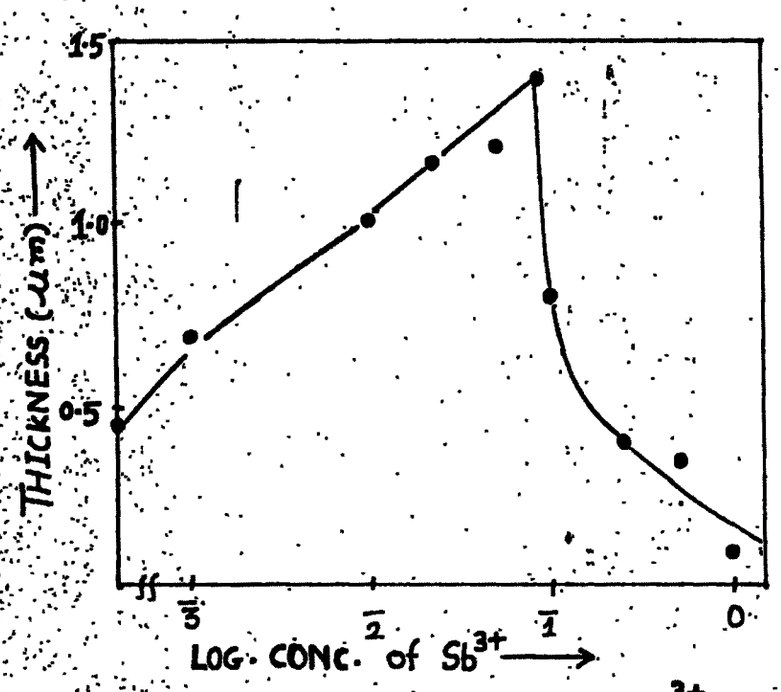

Fig.4.4 Variation of film thickness with log Sb^{3+} concentration.

CdS layer on stationary substrates indicating the powdery, porous, thick, less uniform, and non-reflecting deposits. The effect of speed would seems to imply that the fluid motion prevents adhesion of the precipitated CdS to the surface of the substrate. In this study an intermediate speed of 72 r.p.m. was chosen and kept constant throughout forthcoming studies.

(e) Concentration of basic ingradients.

The above parameters were kept constant and concentration of both cadmium sulphate and thiourea were varied. For low molarities (0.1 to 0.5 M), reflecting and thinner deposits were obtained (0.08 µm to 0.2 µm approximately). The higher molar concentrations gave thick and non-reflecting films. The molarities selected were 1 M each.

f) Cd:S ionic ratio.

Systematic efforts have been taken to fix the Cd:S ion ratio by Pawar and Deshmukh for CdS and Uplane and Pawar [96] for mixed CdS deposits. By thoroughly testing through succesive stages of film and PEC cell properties, they have shown that in purest form of CdS the ionic ratio (Cd:S) approximates 1:1. We have, while processing for the work, started with equimolar contents of both cadmium sulphate and thiourea.

4.3.2 Effect of Sb-doping on film properties.

a) Electrical properties:

The electrical and optical properties of both CdS and CdS:Sb deposits are studied at optimised preparative parameters and conditions. Only the concentration of antimony dopant was changed from 0.005 Wt.% to 1 Wt%. The thickness of the samples was measured and an increase in thickness with antimony doping concentration was observed upto 0.075 Wt%, beyound which it decreases. The dependence of thickness on antimony doping level is shown in fig. 4.4 and can be explained on the basis of the role of the antimony atom as a nucleation centre [43,97]. When glass substrates are dipped into the complex compound of the reactants, a suspension of $Cd(OH)_2$ which acts as a catalytic surface, forms a thin layer on it and decomposes thiourea resulting in CdS film formation. Due to the presence of $Sb(OH)_3$ in a complex suspension, however, nucleation occurs which contributes to the enhancement in the film formation process upto 0.075 Wt% antimony doping level. For higher concentrations the rate of nucleation increases although it may prohibit the entry of Cd^{2+} ions and as a result the thickness decreases [43].

i) Conductivity :

The dc electrical conductivity in dark was measured for all the samples as explained in the

section 4.2.2. The range of working temperature was 300 K to 600 K. It is interesting to note that antimony doping concentration enhances the conductivity which attains its maximum value at 0.075 Wt% and decreases for higher doping levels. The logarithmic variation of the conductivity with temperature for five typical film compositions is shown in fig. 4.5. The plots are linear. The plots are further analysed to calculate the activation energy using the relation [43].

$$\sigma = \sigma_0 \exp(-Ea/KT) \quad \text{.....} \quad (4.1)$$

where, Ea is the activation energy and other terms have their usual meaning. The activation energies are listed in table 4.1. Similar type of results are available in the literature [97,98,100,102,103]. The enhancement in conductivity with antimony doping concentration can be explained on the basis of formation of Cd^+ ions or Cd vacancies being formed for charge compensation because during the film growth trivalent antimony replaces the divalent cadmium and there is possibility of formation of Cd^+ ions rather than the Cd vacancies as antimony and Cd are deposited simultaneously. This helps in increasing the conductivity upto 0.075 Wt% Sb-doping concentration. The charge compensation

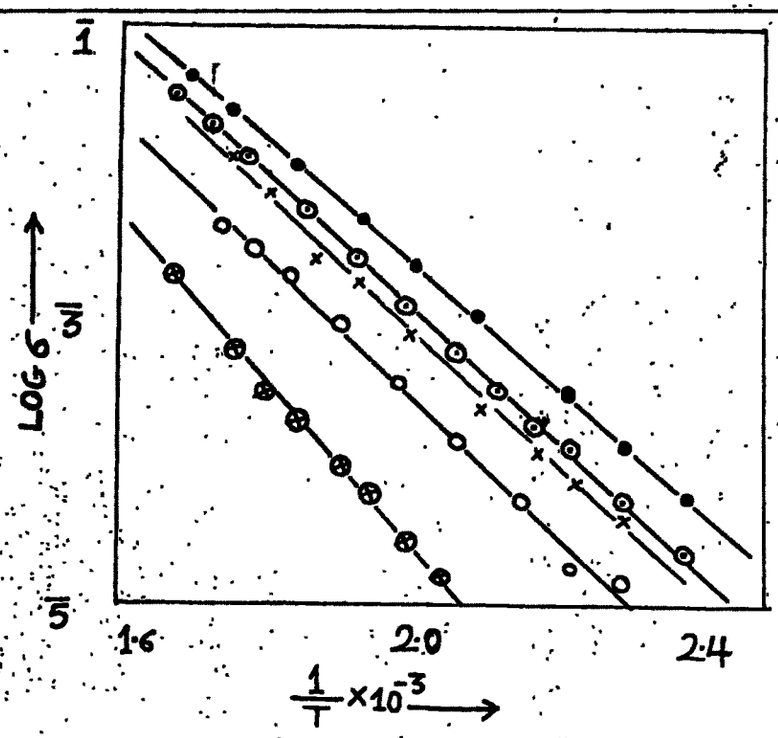

Fig.4.5 Temperature dependence of an electrical conductivity for: ⊙-Pure CdS, O-0.005 wt% CdS:Sb, x-0.01 wt% CdS:Sb, ●-0.075 wt% CdS:Sb, ⊗-0.25 wt% CdS:Sb

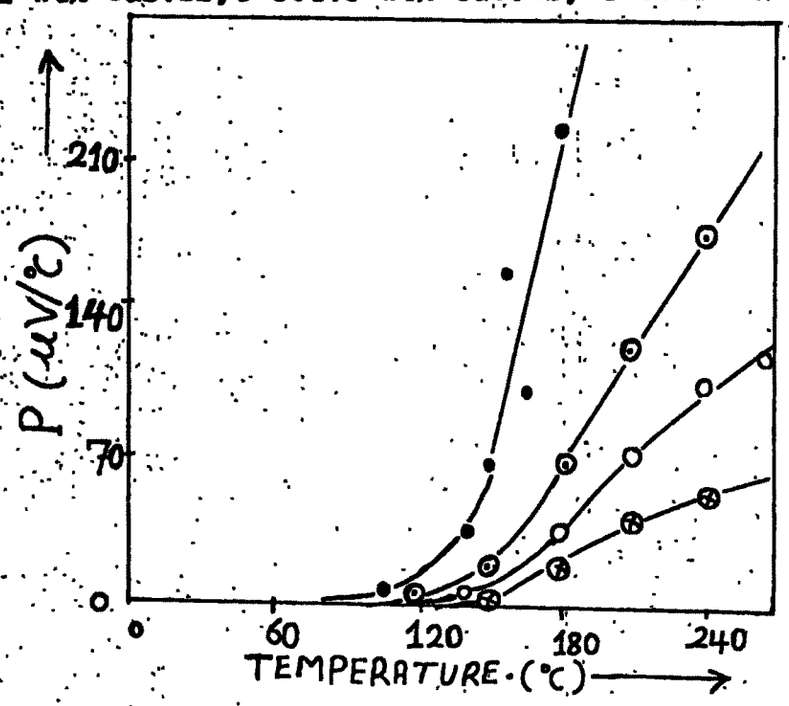

Fig.4.6 Variation of thermoelectric power with temperature for:

⊙-Pure CdS,
O-0.005 wt% CdS:Sb, ●-0.075 wt% CdS:Sb
⊗-0.25 wt% CdS:Sb

process ceases for higher doping concentration which may be due to the migration of antimony atom at an interstitial rather than the vacancy position of Cd [43,97,100].

ii) Thermoelectric power (TEP) :

The thermoelectric power studies have been examined in dark in the temperature range 300 K to 498 K as discussed in section 4.2.2. The polarity of the thermovoltage at the hot end was positive confirming that all the samples are of n-type. Thermoelectric power P is of the order of $\mu V/^{\circ}C$ for all the samples, although it is higher for 0.075 Wt% of CdS:Sb films. The temperature dependence of the thermoelectric power for four typical samples is shown in fig. 4.6.

The relatively superior magnitude of TEP for 0.075 Wt% CdS:Sb deposits can be explained on the similar lines that predicted for PbTe incorporated with Cl^- ions. It is obvious from the previous section that the activation energy is smaller for 0.075 Wt% antimony doped CdS than that of the pure CdS. This ascertains the position of antimony donor levels between the conduction band and the Fermi energy level. Less thermal energy will be required to promote these electrons to conduction band contributing to the increased TEP with increasing temperature. At

higher doping levels, decrease in TEP is observed due to the formation of acceptor levels because of migration of Sb-atoms in the interstitial rather than a vacancy position [100,104]. The carrier concentration (n) and theroelectric power (P) are related as :

$$P = -\frac{K}{q}\left[A + \ln\left\{\frac{2(2m_e^* \cdot KT)^{3/2}}{nh^3}\right\}\right] \quad ..(4.2)$$

where, A is thermoelectric factor (2.4=A for CdS), P the thermoelectric power in μV, n the carrier concentration, h planks constant, m_e^* the effective mass of an electron and t the absolute temperature. Equation (4.2) substitution of various constants simplifies to:

$$\log n = 3/2 \log T - 0.005\, P + 15.7198 \quad .. (4.3)$$

The electron density was calculated by using equation (4.3) and is of the order of 10^{19} cm^{-1} for all the samples, however, it is considerably higher for 0.075 wt% CdS:Sb samples. This is in excellent agreement with the results reported by others [43, 97,100]. The mobility (μ) of the charge carriers is determined from the relation:

$$\mu = \sigma/n.q \quad ..... \quad (4.4)$$

The observed range of mobility is small for both type of samples, however, it is considerably improved for 0.075 wt% antimony doped samples.

This is one of the reasons why conductivity is higher for 0.075 Wt% Sb-doped samples. Fig. 4.7 is a sketch of mobility versus temperature. The intercrystalline barrier height, (T) for all the samples is determined by using the relation;

$$\mu = \mu_0 \exp. (-\phi_B/KT) \quad \ldots\ldots\ldots\ldots \quad (4.5)$$

and are shown in table 4.1. The barrier height (ϕ_B) is found smallest of all for 0.075 Wt% CdS:Sb thin films.

b) Optical properties:

The effect of antimony doping on optical absorption and bandgap was examined in the wavelength range from 4000A° to 9000 A° by employing a photospectrometer as discussed in the section 4.2.3. The optical absorption coefficient (α) is of the order of 10^4 cm^{-1}. Fig. 4.8 shows the wavelength dependence of 'α' for a few samples. From the plots it can be justified that the films show higher absorption on the shorter wavelength side and the presence of an edge. All the samples show some red response and higher cut off wavelength: the cut-off wavelength for CdS and CdS:Sb compositions shifts from 5300 to 6500 A°. This can be satisfactorily understood from the fact that pure CdS films are Cd rich and sulphur deficient. Excess Cd gives rise to donor levels in the bandgap of CdS and larger concentration of Cd in the lattice makes these donor levels degenerate and finally merge into the

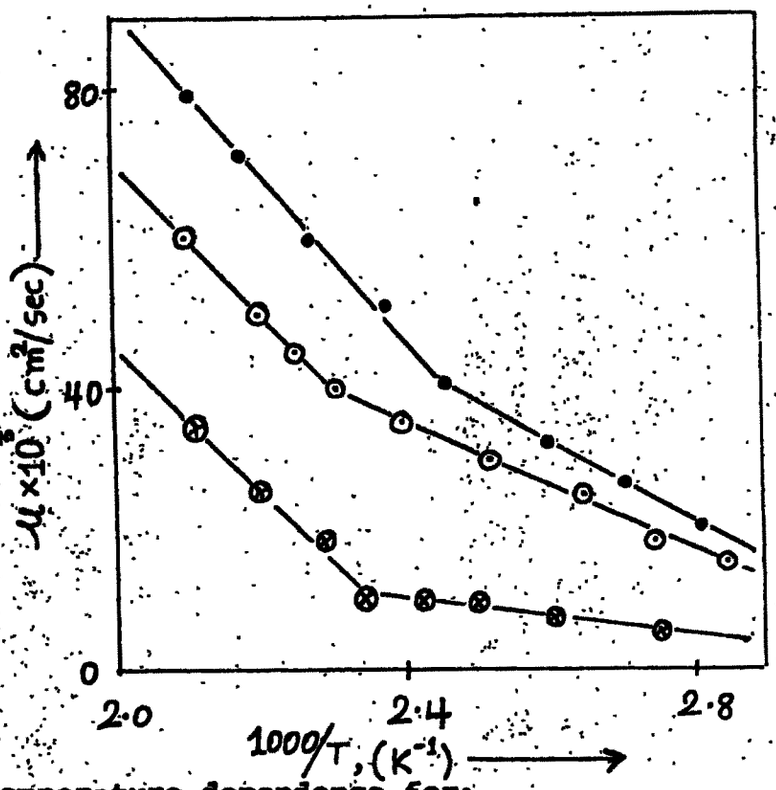

Fig.4.7 Mobility-temperature dependence for: ⊙-Pure CdS, ●-0.075 wt% CdS:Sb, ⊗-0.25 wt% CdS:Sb

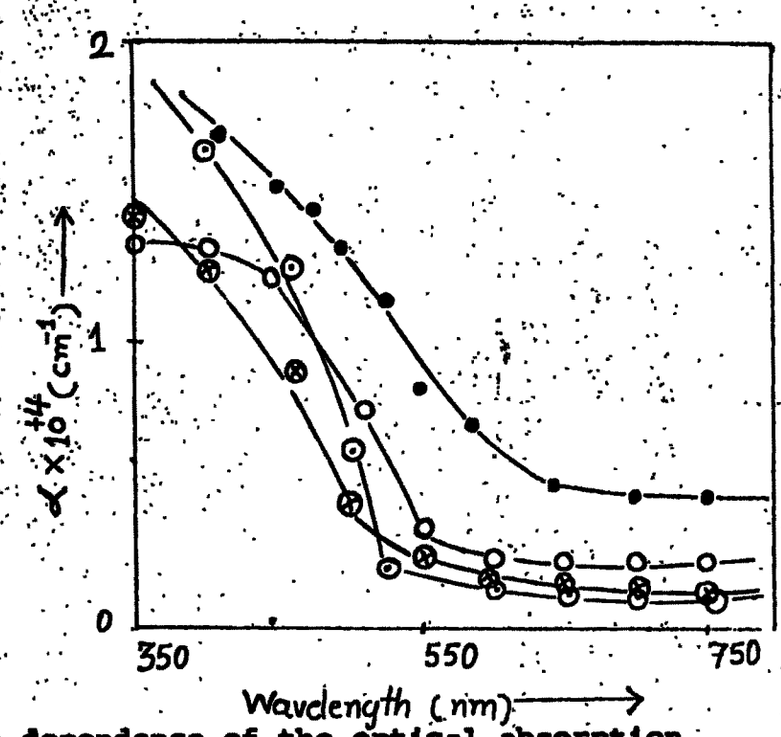

Fig.4.8 Wavelength dependence of the optical absorption coefficient (α) for: ⊙-Pure CdS, O-0.005 wt% CdS:Sb, ●-0.075 wt% CdS:Sb, ⊗-0.25 wt% CdS:Sb

conduction band. Thus an increase in red response and shifting of an absorption edge towards higher cut-off wavelength results. For CdS:Sb samples a higher cut-off and increased red response is observed which can be ascribed to the increased sulphur deficiency. These observations resemble closely with those of others [43,97,98,100]. Fig. 4.9 is a sketch of variation of $(\alpha h\nu)^2$ Vs $h\nu$ from which the band gap energies have been determined. The variation of band gap with the antimony doping level is shown in table 4.1. No systematic variation in band gap is observed with dopent concentration.

4.3.3 Structural properties :

a) XRD Studies :

In order to study the effect of Sb-doping concentration on structural properties, the samples were scanned by a X-ray diffraction techniques in the range of scanning angles between 20° to 80°. The XRD patterns of four typical samples are shown in the fig. 4.10. The XRD patterns consist of peaks corresponding to the different crystallographic planes suggesting the samples to be polycrystalline. This polycrystallinity (imporovement in grain structure) increases as the doping concentration and the additional number of peaks have been observed for 0.075 wt% doping concentration showing that it is

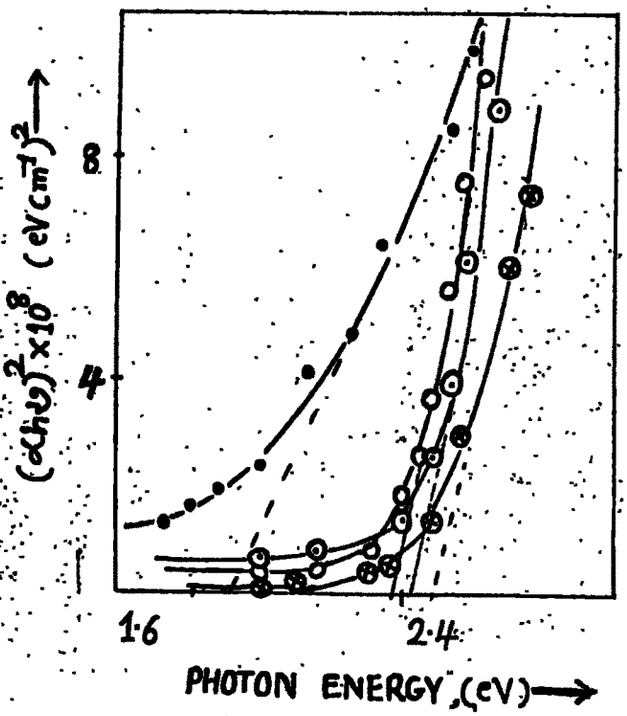

Fig.4.9 Estimation of energy gap for: ⊙-Pure CdS, O-0.005 wt% CdS:Sb, ⊗-0.075 wt% CdS:Sb, ⊗-0.25 wt% CdS:Sb

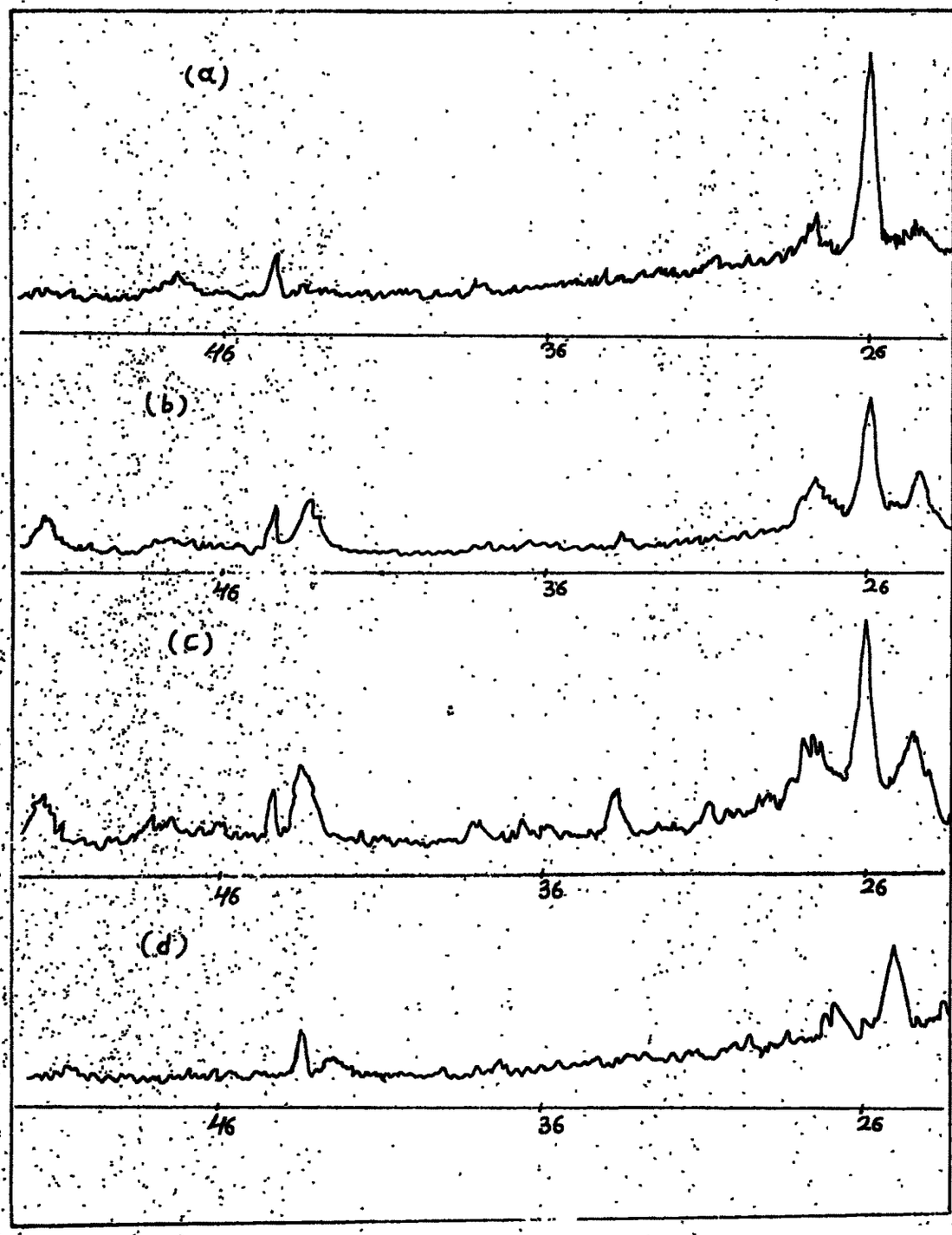

Fig. 4.10 X-ray diffraction patterns for : a) Pure CdS, b) 0.005 wt.% CdS:Sb c) 0.075 wt.% CdS:Sb (d) 0.25 wt.% CdS:Sb samples.

more crystalline than other. For further increase in doping concentration the number of peaks as well as its intensity decreases. This clearly suggests that the crystallinity improves after doping and this exactly agrees with our previous results [43].

The interplanar distance, 'd' values have been calculated and compared with ASTM values. The comparison is shown in Table 4.2. The calculated 'd' values matched closely with the standard values and the CdS deposits are found to be mixture of a hexagonal and a cubic phases [43]. The crystal structure for both the phases was confirmed and it is found that the lattice parameters (average taken for large scanning angles) are as shown in table 4.3. For both the cubic and hexagonal system, the lattice parameter "a" did not varied much with the addition of impurity.

b] SEM Studies :

The crystalline nature of the samples was further tested by SEM micrographs. It has been seen that the films are ploycrystalline with defined grain boundaries. The SEM micrographs showing grannular structure of both type of samples are shown in fig. 4.11. for four typical samples. The crystallinity of the samples is found increased with low level of doping concentration. The grain size is improved after doping, well defined grain structure is observed for 0.075wt% CdS:Sb

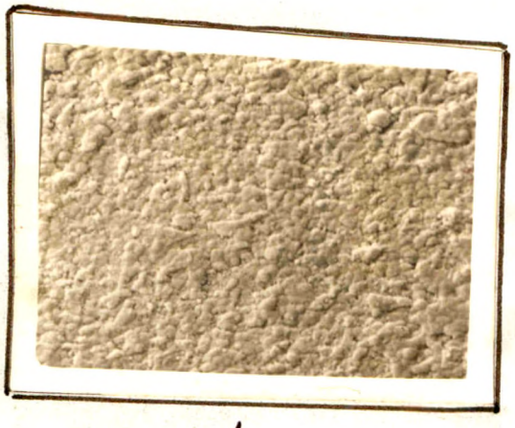

1

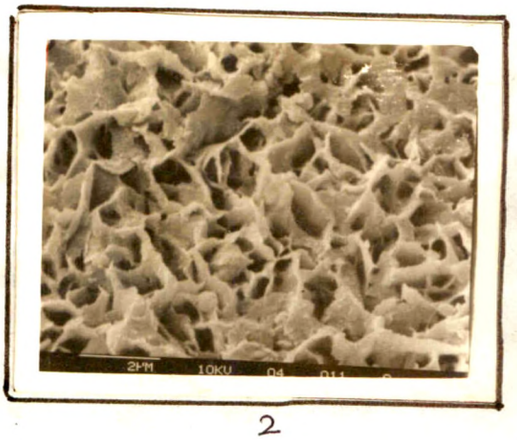

2

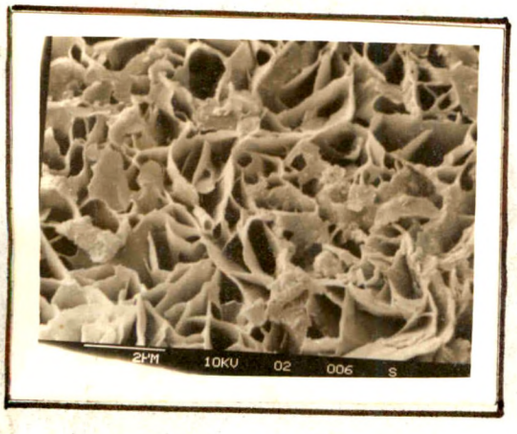

3

4

Fig.4.11 SEM micrographs of four typical samples,1)pure CdS 2) 0.05 Wt.% CdS:Sb (3) 0.075 wt.% CdS:Sb, and 4) 0.25 wt% CdS:Sb samples.

composition and a decrease in grain size is observed for higher doping concentrations. This is in good agreement with our previous reported results.

Table 4.1

Some parameters of the doped and undoped CdS thin films.

Sr.No.	Doping Concentration Sb wt%	Thickness μm	Activation Energy (eV)	Eg (Opt) eV	Eg (therm) eV	ϕ_B eV
1	0 (pure CdS)	0.45	0.97	2.47	1.94	0.93
2	0.005	0.73	0.94	2.40	1.88	0.82
3	0.010	1.03	0.90	2.31	1.80	0.71
4	0.025	1.17	0.99	2.00	1.98	0.87
5	0.050	1.21	0.93	1.92	1.86	0.66
6	0.075	1.44	0.83	1.85	1.66	0.54
7	0.100	0.77	0.94	1.70	1.88	0.58
8	0.250	0.41	1.15	2.43	2.30	0.89
9	0.500	0.36	0.88	2.86	1.76	1.13

Table 4.2

Comparison of relative intensity (I) and interplanar distance (d) vs angle of diffraction for different samples

Sr. No.	Sample	2θ	"d" ASTM	"d" Observed	I/Imax	Plane (hkl) Hexa	Plane (hkl) Cubic
		23.100	-	3.850	37.200	-	-
		24.400	3.590	3.640	38.500	100	-
		26.200	3.360	3.400	100.000	002	111 (β)
1	CdS	27.700	3.160	3.220	41.030	101	-
		38.800	2.900	2.900	25.600	-	200 (β)
		44.500	2.058	2.038	24.300	-	220 (β)
		47.600	1.900	1.910	23.070	103	-
		24.400	3.590	3.640	64.440	100	-
		26.100	3.360	3.400	100.000	002	111 (β)
	CdS : Sb	27.800	3.160	3.200	60.000	101	-
2		30.600	2.900	2.910	40.000	-	200 (β)
	(0.01 wt%	38.200	2.450	2.360	22.220	102	-
	Sb)	43.400	2.070	2.080	24.440	110	-
		44.400	2.058	2.040	40.000	-	220 (β)
		51.600	1.760	1.760	17.780	112	311 (β)

		24.500	3.590	3.630	55.520	100	-
		27.100	3.340	3.270	100.000	002	111 (β)
		28.600	3.160	3.120	55.520	101	-
		31.900	2.900	2.800	23.880	-	200 (β)
		34.700	-	2.580	28.360	-	-
	CdS : Sb	36.800	2.450	2.440	14.930	102	-
3		37.600	-	2.400	17.920	-	-
	(0.075wt%	39.000	-	2.300	16.420	-	-
	Sb)	44.600	2.050	2.030	41.800	110	220 (β)
		45.400	-	1.990	29.860	-	-
		47.000	-	1.930	16.420	-	-
		48.500	1.890	1.880	19.410	103	-
		49.200	-	1.850	20.900	-	-
		52.600	1.731	1.740	31.350	201	311 (β)
		24.400	3.590	3.640	56.520	100	-
		26.000	3.360	3.420	100.000	002	111 (β)
	CdS : Sb	27.600	3.160	3.230	54.350	101	-
4		33.800	-	2.650	17.390	-	-
	(0.1 wt%	43.300	2.070	2.080	36.960	110	-
	Sb)	44.400	2.058	2.040	32.610	-	220
		51.600	1.760	1.760	30.440	112	311 (β)

Table 4.3

Determination of lattice parameters for four typical samples

Sr. No.	Phase	Doping Concentration	Lattice parameters		
			a Å	b Å	c Å
1	Hexagonal (a = b ≠ c)	0	4.14	4.14	6.76
		0.01 wt% Sb	4.18	4.18	6.82
		0.075 wt% Sb	4.20	4.20	6.56
		0.1 wt% Sb	4.19	4.19	6.85
2	cubic (a = b = c)	0	5.82	-	-
		0.01 wt% Sb	5.82	-	-
		0.075 wt% Sb	5.73	-	-
		0.1 wt% Sb	5.82	-	-